*J. Fluid Mech.* (1995), *vol.* 304, *pp.* 321–342



# A two-dimensional cusp at the trailing edge of an air bubble rising in a viscoelastic liquid

By Y. J. LIU, T. Y. LIAO AND D. D. JOSEPH

Department of Aerospace Engineering and Mechanics, University of Minnesota, Minneapolis, MN 55455, USA

(Received 31 October 1994 and in revised form 24 July 1995)

When an air bubble rises in a viscoelastic fluid there is a critical capillary number for cusping and jump in velocity: when the capillary number is below critical, which is about 1 in our data, there is no cusp at the tail of a (smooth) air bubble. For larger volumes, a two-dimensional cusp, sharp in one view and broad in the orthogonal view, is in evidence. Measurements suggest that the cusp tip is in the generic form $y = ax^{2/3}$ satisfied by analytic cusps. The intervals of volumes for which dramatic changes in air bubble shape take place is very small and the two to ten fold increase in the rise velocity which accompanies the small change of volume could be modelled as a discontinuity. A second drag transition and an orientational transition occurred when $U/c > 1$ where $U$ is the rise velocity of an air bubble and $c$ is the shear wave speed. For $U/c < 1$, $U$ is proportional to $d^2$, where $d$ is the equivalent diameter for a sphere of diameter $d$ having the same volume, and when $U/c > 1$ then $U$ is proportional to $d$ and the Deborah number does not change with $U$. Moreover the bubble shapes when $U/c < 1$ are overall prolate (with or without a cusped tail) with the long side parallel to gravity, in contrast to the oblate shapes which are always observed in Newtonian fluids and in viscoelastic fluids with $U/c > 1$ when inertia is dominant. The formation of cusps occurs in all kinds of columns of different sizes and shapes. Cusping is generic but the orientation of the broad edge with respect to the sidewalls is an issue. There is no preferred orientation in columns with round cross-sections, or in the case of walls far away from the rising bubble. In columns with rectangular cross-sections, three relatively stable configurations can be observed: the cusp can be observed in the wide window and the broad edge in the narrow window; the cusp can be observed in the narrow window and the broad edge in the wide window or, less frequently, the broad edge lies along a diagonal. These orientational and drag alternatives are directly analogous to those which are observed in the settling of long or broad solid bodies (Liu & Joseph 1993).

## 1. Introduction

An astonishing two-dimensional cusp with a cusp point in one view and a spade edge in the orthogonal view can form at the tail of an air bubble rising in a viscoelastic fluid (Hassager 1979). It is hard to imagine how such a singularly asymmetric feature could arise in situations which in every respect suggest that an axisymmetric shape should prevail. New observations and measurements of the cusping of air bubbles rising in a viscoelastic liquid are reported here. The broad edge is flat like a spade, arched like an axe, pointed like an arrow or flat and tilted like a guillotine, depending on conditions (see figure 1).

The results collected in this paper are closely related to the formation of cusps

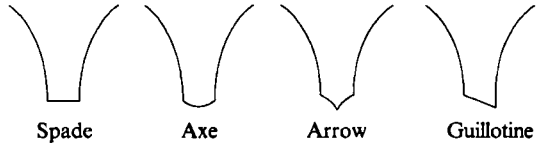


FIGURE 1. Shapes of the broad edge of the two-dimensional cusps.

induced at the free surface of a viscous liquid by a rotating cylinder which is partially immersed in the reservoir of liquid (Joseph *et al.* 1991). The liquid forms a thick coat on the surface of the cylinder and the coat of liquid rotates nearly as a rigid body. The liquid is pulled out of the reservoir on one side and is plunged into the reservoir on the other side where it forms an apparent cusp at a critical capillary number $Ca = U\eta/\sigma$ where $\eta$ is the viscosity and $\sigma$ is the surface tension. Joseph *et al.* (1991) showed that the cusp is given locally by $y = ax^{2/3}$ when surface tension is neglected. Jeong & Moffatt (1992) solved a model problem exactly and they showed that surface tension rounds the cusp tip but that the radius of curvature at the cusp tip is exponentially small, of the order of hundreds of angstroms at capillary numbers of order one. Moreover, the shape of the free surface near the rounded cusp is universally $y = ax^{2/3}$, independent of surface tension. The capillary number criterion for effective cusping of Jeong & Moffatt (1992) is in broad agreement with the observations of Joseph *et al.* (1991) and with their own observations. Joseph (1992) argued that the cusp equation is just the one which satisfies $F(x, y) = 0$ for an analytic function $F$ at lowest order (generically); that is

$$0 = F(x,y) = \tfrac{1}{2}F_{xx}(0,0)\,x^2 + \frac{1}{3!}F_{yyy}(0,0)\,y^3 + O[x^{7/3}] \tag{1}$$

in a coordinate system in which $F_{xy}(0,0) = 0$. From this point forward, we shall adopt the convention that a 'two-dimensional cusp' is an apparent or effective cusp with a small rounded tip whose radius perhaps reduces to molecular dimension at high capillary numbers, as in the analysis of Jeong & Moffatt.

Joseph *et al.* (1991) showed that cusping occurs more abruptly in viscoelastic liquids with well-defined critical capillary numbers and well-defined cusps at the point of inception. Joseph's (1992) local analysis of cusping of a second-order fluid without surface tension is consistent with the generic cusp shape $y = ax^{2/3}$ but the flow field is more singular than in the Newtonian case, consistent with the observations. The critical capillary number for cusping of viscoelastic liquids ranges from 0.48 to 9.25 deviating to both sides of the critical value for Newtonian liquids.

In the present series of experiments on rising bubbles we see cusp formation in Newtonian liquids only when the column is tilted, and no cusping for free rising bubbles. Otherwise, air bubbles rising in viscoelastic liquids differ from those in Newtonian liquids in several ways. First, they are prolate with the long side parallel to gravity rather than oblate with the long side perpendicular to gravity. When the rise velocity is larger than the shear wave speed, inertia again dominates as in a Newtonian fluid. Depending on the bubble volume, the shapes of a rising bubble in viscous Newtonian fluids will, roughly speaking, go from spherical to oblate spherical to that of a spherical cap (a more varied range of regimes can be found in Bhaga & Weber 1981). But, bubble shapes in many viscoelastic fluids range from spherical to prolate spherical to that with a trailing cusp. Trailing cusps form at a critical capillary number initiating a sudden change in shape of the bubble accompanied by a sharp reduction in drag and a large increase of the terminal rise velocity. Trailing cusps on gas bubbles and liquid drops and other shapes have been reported in experiments by Philippoff

(1937), Warshsy *et al.* (1959), Mhatre & Kintner (1959), Astarita & Apuzzo (1965), Barnett, Humpherey & Litt (1966), Calderbank (1967), Calderbank, Johnson & Loudon (1970), Leal, Skoog & Acrivos (1971), Zana & Leal (1978), Hassager (1979, 1985) and Coutanceau & Hajjam (1982). Hassagar (1979) was the first to show that this trailing cusp is actually two-dimensional with a cusp edge in one direction and a spade edge in the orthogonal direction. Joseph & Renardy (1993) attempted to relate the bubble cusp to the free surface cusp induced by rotating cylinders. According to the present study, their hypothesis is found to be valid.

Hassager (1979) reported an experiment which reveals an unexpected phenomenon, a 'negative wake': the fluid behind the rising bubbles is actually flowing away from the bubbles in polymeric liquids. The negative wakes in polymeric liquids can be found not only behind bubbles also behind solid spheres according to Sigli & Coutanceau (1977), Bisgaard & Hassager (1982), and Bisgaard (1983). Such wakes have recently been computed by Feng *et al.* (1995) and by Joseph & Feng (1995). The existence of a negative wake suggests extensional forces tending to pull out a cusp against the restraining action of surface tension.

Chilcott & Rallison (1988) modelled a dilute polymer solution as a suspension of dumbbells with finite extensibility. Flows past cylindrical and spherical surfaces at low Reynolds number were calculated using a no-slip (for a solid body) and a zero-tangential-stress (for a spherical or cylindrical bubble) boundary condition at the body surface. They found that at large Deborah numbers the polymer is most highly stretched in thin regions at the rear of the body and suggested that the stresses could overcome surface tension to produce cusped or pointed tips and a change of shape accompanied by a marked change of drag.

Noh, Kang & Leal (1993) computed the steady deformation of an axisymmetric bubble in the creeping flow limit and called attention to a tendency to exhibit a transition from a spherical to a cusped shape as the capillary number increases. Figures 15 and 20 in their paper show a tendency to form a cusp as capillary number increases from 0 to 0.5 (limited by the code). Their results are not inconsistent with our experimental observations of cusping at a critical capillary number of approximately unity, except that an axisymmetric cusp is never seen in experiments.

A gas bubble rising in a viscoelastic liquid also exhibits a discontinuity in the terminal velocity at a critical cusping volume (see Astarita & Apuzzo 1965; Calderbank *et al.* 1970; Leal *et al.* 1971; Zana 1975; Acharya, Mshelkar & Ulbrecht 1977; Clift, Grace & Weber 1978; De Kée, Carreau & Mordarski 1986; Bird, Armstrong & Hassager 1987). Other researchers, such as Garner, Matrus & Jensen (1957), Warshey *et al.* (1959), Fararouri & Kintner (1961), Barnett & Humpherey (1966) have also noted a smaller and less abrupt transition in terminal velocity of liquid drops in viscoelastic fluids at some critical volume.

Astarita & Apuzzo (1965) suggested that the discontinuity in the rise velocity is an effect of surface-active impurity which immobilize small bubbles. They assumed that the observed transition is due to a transition in the boundary condition from no-slip for small bubbles in the Stokes regime to free surface conditions for larger bubbles in the Hadamand–Ryligynski regime. Leal *et al.* (1971) compared terminal velocities for gas bubbles and glass spheres in an aqueous polyacrylamide: no velocity discontinuity was observed for the glass sphere, but one was observed in the gas bubble. They concluded that these observations supplied strong evidence for the hypothesis of Astarita & Apuzzo. Calderbank *et al.* (1970) studied bubble shapes and terminal velocities in polymer solutions and expressed general approval of the hypothesis without giving any direct or quantitative evidence. Acharya *et al.* (1977) suggested that

the polymer molecules might act as the surfactant required to make the slip to no-slip hypothesis work. Bird *et al.* (1987) noted that the surfactant could accumulate at the trailing edge of a closed bubble but would be swept off a cusped knife edge by the flow. None of the aforementioned authors have shown that surface-active agents are present on the gas bubbles they studied, nor have any other quantitative supporting data been given.

We believe that the jump in the velocity is due to the reduction in the drag which follows rapidly from the change of shape due to cusping near a critical capillary number with or without surfactants. There are no published examples of a discontinuity in the bubble rise velocity without a simultaneous change of shape. However De Kée *et al.* (1986) did not find a velocity discontinuity in the rise velocity of air bubbles in 1% CMC and 1% PAA solutions for which cusp-like tails are clearly evident. Their result seems to contradict the results of Acharya *et al.* (1977) and Leal *et al.* (1971) who did find small velocity jumps in similar liquids at the point of apparent cusping.

## 2. Experiments

### 2.1. *Setup*

The experimental setup is shown in figure 2 and is explained in the caption and the following text.

To obtain quantitative data from experiments on air bubbles rising in a liquid, the first problem that has to be solved is the control and measurement of the volume of the bubbles. We have developed an 'equal volume' method for this purpose. Each of our test columns has the specially designed ends shown in figure 2. The column is extended at both ends with two short tubes in divergent holes in the end covers. One tube is closed with a rubber hat, the other is linked to a scaled syringe through a valve. The filled column is vertical with the syringe at the bottom as shown in figure 2. The chamber between the syringe and the valve is filled with test liquid during the installation. The pressure at the top of the column is balanced against atmosphere pressure by manipulating an injection needle in the rubber hat until there is no liquid coming out of the column and no air going in. Then, the valve is opened at the bottom and liquid is sucked out of the column using the syringe; air will enter the column from the needle at the top. Since the volume of the column is a constant, the volume of the air bubble is expected to equal the volume of the liquid in the syringe. At this stage, the needle is pulled out and the valve is closed, leaving an air bubble of known volume in the closed column. We estimate that the volume is correct to within 5%. Volumes of air bubbles of less than 0.05 $cm^3$, which are mostly spherical or slightly elliptical, are determined from scaled pictures.

The 'equal volume' method just described does not work well in large columns. In these, one finds a sensible compressibility induced by the large liquid mass acting on larger column walls of reduced rigidity. For example, a $3 \times 4 \times 46.5$ in. column with wall thickness of 0.22 in. has a compressibility of about 1 $cm^3$. For large columns we used the two-chamber device shown in figure 3 in which the large test column is attached to a small bubble-generating chamber by a valve. The small chamber works by the 'equal volume' method described in the previous paragraph. Both chambers are filled with test liquid and isolated from each other by the closed valve. An air bubble of known volume is then generated in the small chamber by the 'equal volume' method and is transferred to the test chamber by opening the valve.

The holes on the end covers are tapered to prevent the entering air bubble from breaking. The heavy metal base is levelled by screws to ensure that the column is

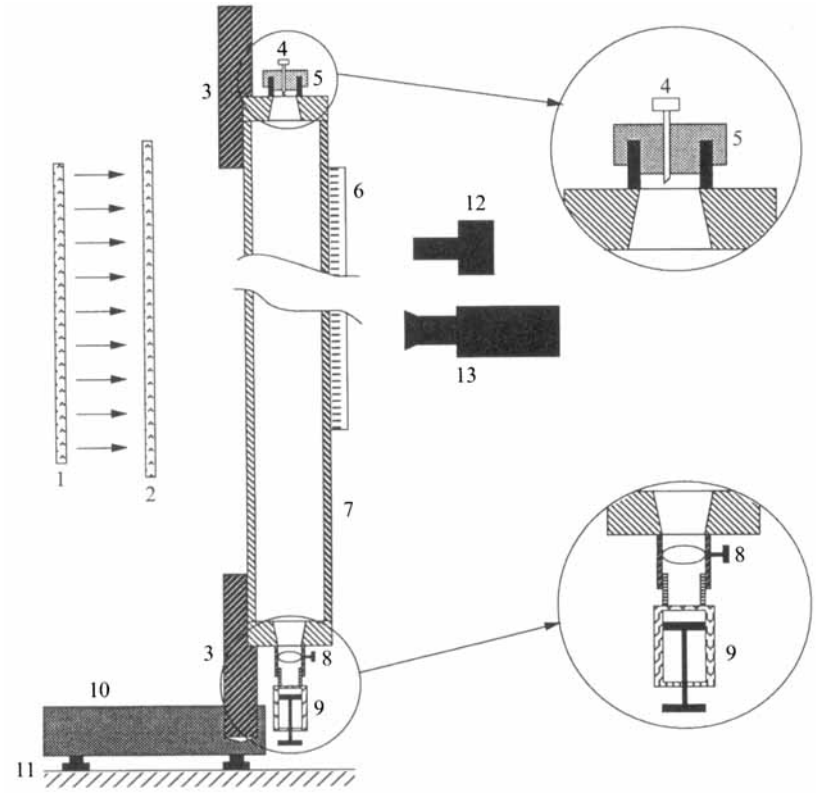


FIGURE 2. Experimental setup. The test column (7) is fixed at each end with a rod (3) which can be put into a hole in the heavy metal base (10) to ensure that the column is vertical. The level is adjusted with three screws (11) under the base. The volume of the air bubble is controlled and measured by an 'equal volume' method. The column is filled with liquid and the pressure at the top of the column is balanced against the atmosphere. An injection needle (4) is put into the column through the rubber cover (5) at the top of the column. Now, the valve (8) is opened and liquid is sucked out of the column using a scaled syringe (9); air then enters the column from the needle. The volume of the air bubble is ideally equal to the volume of the liquid in the syringe. The needle is then pulled out and the valve is closed. Measurements can be conducted repeatedly by turning the column upside down. A light source (1) is put behind the column with a plate light diffuser (2) in between. A ruler (6) is mounted at the centre of the sidewall in the same plane as the rising air bubble. A photo camera (12) and video camera (13) are used to take pictures.

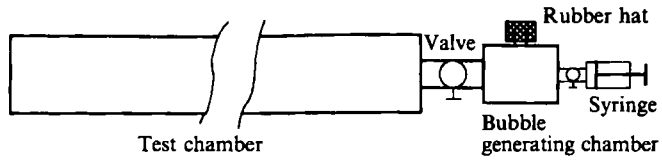


FIGURE 3. Two-chamber system. The test air bubble is generated in a separate small chamber which is connected to the test column through a valve.

vertical when one of the rods (3) in figure 2 is put into the hole in the base. For the large column, we placed an orthogonal frame above the levelled base. When the column is set on the base against the frame, it is vertical.

We used still photography to accurately measure the bubble and cusp. A planar light was set behind the test column. A light-diffusing opaque plate between the light source

| Column | Geometry | Inner dimensions (in.) | Purpose | Liquid tested |
|---|---|---|---|---|
| 1 | Rectangular | 1 × 1.63 × 28 | Observation | S1 solution |
| 2 | Square | 1 × 1 × 24 | Observation | S1 solution |
| 3 | Round | 2.76 × 29 | Observation | 2% aqueous polyacrylamide |
| 4 | Rectangular | 1 × 1.5 × 28 | Observation and measurement | 1 and 1.5% aqueous polyox, pure glycerin |
| 5 | Square | 1.5 × 1.5 × 28 | Observation and measurement | 1.5% aqueous polyox |
| 6 | Round | 1.5 × 28 | Observation and measurement | 1.5% aqueous polyox |
| 7 | Rectangular | 3 × 4 × 46.5 | Observation and measurement | 1.5% aqueous polyox |
| 8 | Round | 0.8 × 8 | Observation | Aqueous polyox, STP glycerin |
| 9 | Round | 2 × 14 | Observation | STP |
| 10 | Square | 10 × 10 × 15 | Observation | 0.85% aqueous polyox |

TABLE 1. Geometry and dimensions of the bubble columns used in the experiments

| Liquid | $\rho$ (g cm$^{-3}$) | $\eta_0$ (Pa s) | $\kappa$ | $n$ | $\hat{\beta}$ (g cm$^{-1}$) | $c$ (cm s$^{-1}$) | $\sigma$ (dyn cm$^{-1}$) |
|---|---|---|---|---|---|---|---|
| 0.85% aqueous polyox (WSR 301) | 1 | 5.75 | 2.93 | 0.43 | 90.6 | 12.2 | 60.9 |
| 1.0% aqueous polyox (WSR 301) | 1 | 7.65 | 3.97 | 0.42 | 108 | 15.0 | 61.2 |
| 1.5% aqueous polyox (WSR 301) | 1 | 17.3 | 5.71 | 0.44 | 132 | 20.3 | 63.3 |
| 2% aqueous polyox (WSR 301) | 1 | 35 | | | | | |
| S1 | 0.875 | 8.06 | 7.14 | 0.62 | 11.8 | 72.4 | |
| STP | 0.86 | 18.0 | 17.8 | 0.85 | 0.97 | 286 | |
| Pure glycerin | 1.26 | 1.44 | | | | | |
| 70% glycerin in water | 1.18 | 0.023 | | | | | |

TABLE 2. Summary of material parameters: density $\rho$, viscosity $\eta = \kappa\dot{\gamma}^{n-1}$ where $\dot{\gamma}$ is the shear rate in s$^{-1}$, climbing constant $\hat{\beta}$ measured on a rotating-rod viscometer, the shear wave speed $c$ measured on the shear wave speed meter, and surface tension $\sigma$ measured on a spinning-drop tensiometer. Note that the power-law parameters are fitted for moderate shear rates, and are not good for low shear rates. $\eta_0$ is the zero-shear viscosity and it is not equal to $\kappa$

and the column was used to remove unwanted reflections. A ruler was mounted on the sidewall at the centreplane where air bubbles rise. Ruler scales appearing in the photographs can be used to determine the real dimensions of an air bubble. We enlarged the pictures to take the measurements. For large air bubbles which rise with

higher speeds, a video camera was also used. The rise velocity of an air bubble was measured with a stop watch with 0.001 s accuracy. For large bubbles, rise velocities were also measured using a video system with a playback speed of 1/30 second per frame. The cusp curvature was measured from image processing photographs scanned into a computer. The ten bubble columns listed in table 1 were used for observations and measurements.

### 2.2. *Test liquids*

These are listed together with measured properties in table 2 and have been discussed and characterized in great detail in Joseph *et al.* (1994). The polyox solutions are standard test liquids with appreciable normal stress and sensible, if not large, shear thinning. S1 and STP do not shear thin appreciably at low and moderate rates of shear, but S1 is much more mobile and has larger normal stresses than STP.

## 3. Rise curves and overall bubble shape

In our experiments, the bubble volume is controlled at prescribed values. An equivalent diameter $d$ is defined by the sphere with the same volume. The terminal velocity $U$ of a rising gas bubble is determined by a balance of weight and drag. For creeping flow, the drag is proportional to $Ud$ and the buoyancy to $d^3$; hence $U$ is proportional to $d^2$ in creeping flow.

A rise curve is given by a plot of $U$ versus bubble volume; these are primitive data. However, it is more instructive to look at instead at four other rise curves, all proportional to $U$, in which different physical effects may be more readily understood. In figure 4, we have plotted rise curves for

$$Ca = U\eta_0/\sigma \quad \text{(Capillary number)}, \tag{2}$$

$$Re = \rho Ud/\eta_0 \quad \text{(Reynolds number)}, \tag{3}$$

$$M = U/c \quad \text{(Viscoelastic Mach number)}, \tag{4}$$

$$De = u\lambda/d \quad \text{(Deborah number)}, \tag{5}$$

where $\lambda = \eta_0/c^2\rho$ is obtained from shear wave speed measurements. The last three parameters are not independent because

$$Re\,De = M^2. \tag{6}$$

These rise curves are presented for the two polyox solutions for which we could obtain a terminal $U > c$ which was not too large to measure. The only way to increase the bubble velocity for a given gas and liquid is to increase the bubble volume and it will not be possible to raise $U$ above $c$ if the gas bubble is retarded by the close walls.

Capillary number versus bubble volume curves for air bubbles rising in 1.5% aqueous polyox in four different bubble columns are shown in figure 5. Two transitional regimes can be identified in the rise curves. The first corresponds to a rapid increase in the terminal velocity apparently due to the formation of a cusp at a capillary number near unity. The sudden rise of velocity is a critical event associated with the change to a cusped shape. The slopes of the rise curves do not change after the velocity rise in our experiments or the others in the literature. This implies that $U \propto d^2$ holds before and after the first transition. We get a 'one time' decrease of drag around the point of cusping.

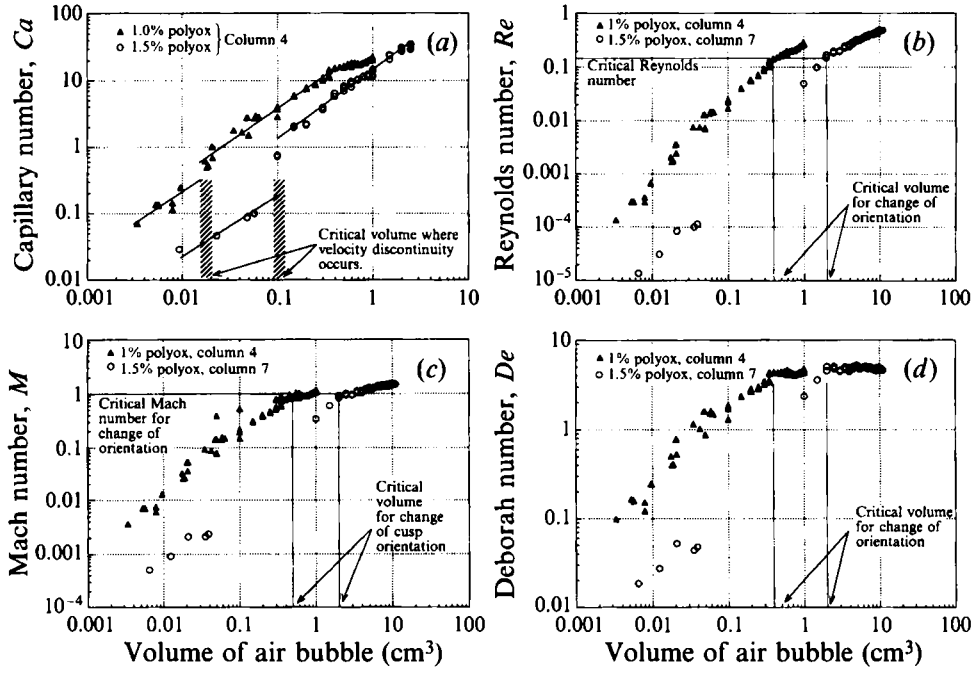


FIGURE 4. Rise curves: volume of air bubble *vs.* (*a*) *Ca*, (*b*) *Re*, (*c*) *M* and (*d*) *De*. A terminal velocity $U > c$ could not be achieved in the 1.5% polyox solution when the column 4 diameter was too small but we did obtain bubbles of large volume with $U > c$, but not too large to measure in the larger column 7. Critical volumes for discontinuities of value and slope of the rise curves are indicated.

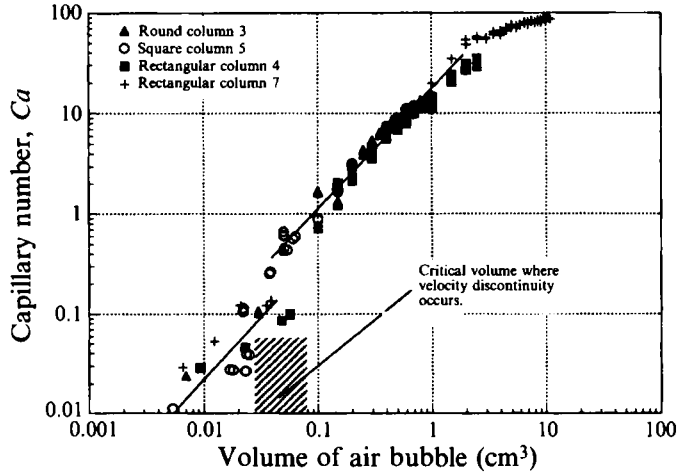


FIGURE 5. The capillary number versus volume for an air bubble rising in 1.5% aqueous polyox in four of the columns listed in table 1. A rapid variation of the rise velocity occurred more or less on $Ca = 1$ curves over a small interval of volumes. The magnitude of the jump and the intervals of the fast variation, for $Ca = 1$, depend on the column used.

The second transition occurs for $M \approx 1$, $Re \approx 0.2$ and $De = M^2/Re \approx 5$. $De \approx 5$ is constant, independent of $d$ for $d$ larger than the critical value for the change of slope; hence $U\lambda/d \approx 5$ shows that, after the second transition, $U$ proportional to $d$ replaces $U$ proportional to $d^2$; the second transition leads to increased drag.

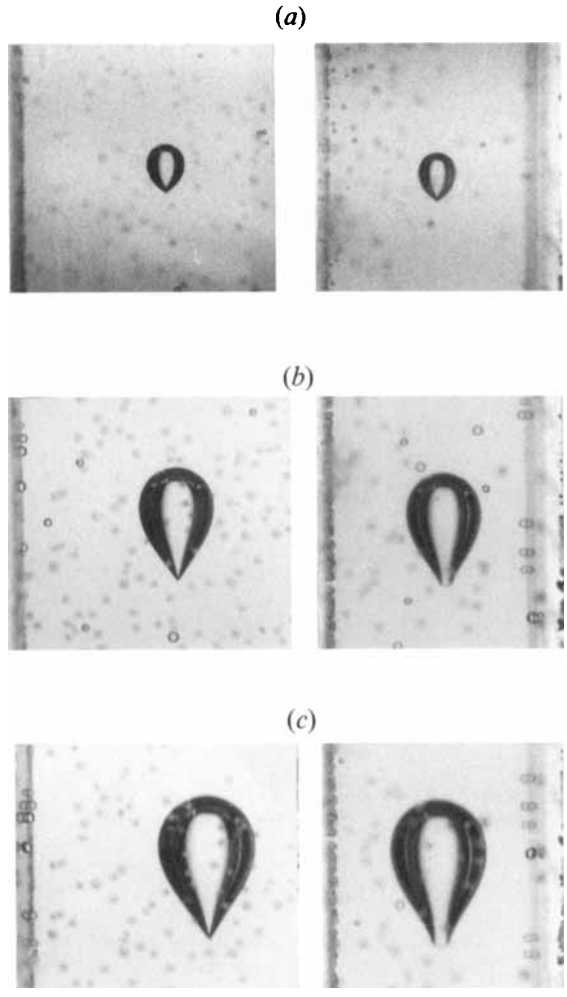


FIGURE 6. Cusped bubbles rising in a 1.5% polyox solution at subcritical values $U < c$, with volumes (*a*) 0.1 cm$^3$, (*b*) 0.8 cm$^3$ and (*c*) 1.5 cm$^3$. Rectangular column 4 was used, and two mutually orthogonal views are shown. These prolate shapes can be identified with subcritical points on the rise curves. The orientation of the cusp edge is such that the broad edge is parallel to the narrow wall of the rectangular column. The cusp edge does not look like a true cusp, though under magnification it may have a cusp like appearance with a rounded tip of small radius.

Two other effects are associated with the transition to supercritical flow. The first is the dramatic change in the orientation of the cusp edge which will be discussed in the following section. The second effect is the change from prolate shapes when $M < 1$ to oblate shapes when $M > 1$. These two effects are evident from the photographs in figure 6 for $M < 1$ and in figure 7 for $M > 1$. Oblate shapes of rising gas bubbles like those shown in figure 7 are not observed in Newtonian fluids (cf. figure 17). It seems probable that the increase in the drag is a consequence of the change of shape to oblate as the Mach number is increased past 1.

An air bubble will change shape from spherical to oblate in a Newtonian liquid as its volume increases, but will change shape from spherical to prolate in a viscoelastic liquid. The same reversed pressure forces which align a long body sedimenting slowly in a viscoelastic fluid with the stream (Feng *et al.* 1995) will pull a spherical bubble into

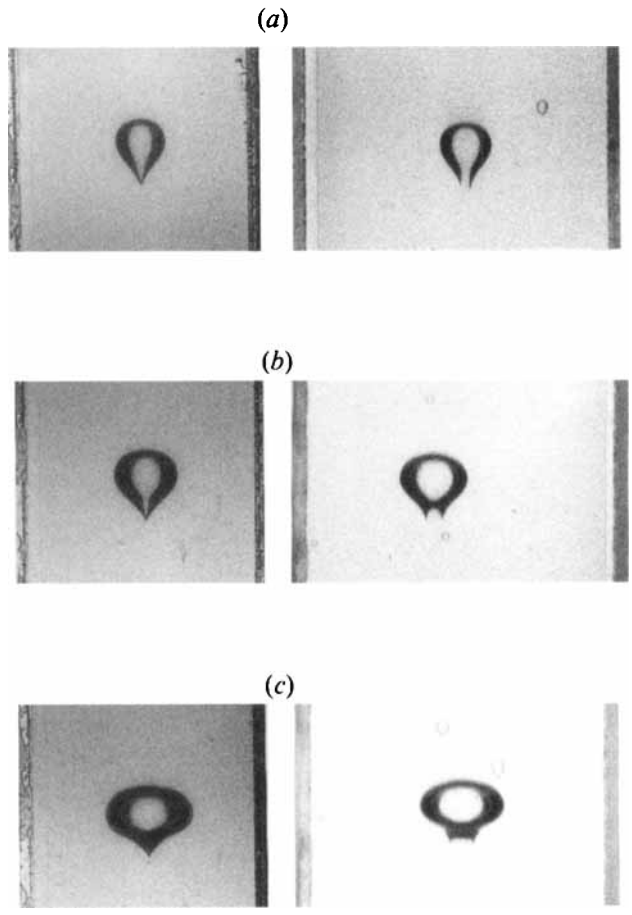


FIGURE 7. Cusped bubbles rising in 1.5% aqueous polyox solution at supercritical values $U > c$, with volumes (*a*) 2 cm$^3$, (*b*) 6 cm$^3$ and (*c*) 10 cm$^3$. The larger rectangular column 7 was used. These oblate shapes can be identified with supercritical points on the rise curves. The broad edge of the cusp is parallel to the wide wall of the rectangular column.

prolate form. Further increases of the volume of the air bubble rising in a viscoelastic liquid lead to the formation of a cusp tail. We measured the maximum horizontal diameter $d$ and height $h$ of the bubble and the length $l_c$ of the two-dimensional cusp. Figure 8 shows the relation between the horizontal diameter, the height and the bubble volume (equivalent diameter $d_e$). When the bubble diameter is, say, less than 0.3 cm it is perfectly spherical. When the volume of the bubble is further increased ($d > d_1$), the bubble changes shape from spherical to prolate with diameter less than and height greater than the equivalent diameter for a sphere with the same volume. Further increases of bubble volume to an equivalent diameter $d_2$ lead to the formation of a two-dimensional cusp at the rear of the bubble and a rapid increase in the rise velocity. As the equivalent diameter of the bubble is further increased past a value $d_3$, the shape change from spherical to prolate slows down and the bubble starts to become oblate. This change to oblate shape occurs in the region of volumes for which the viscoelastic Mach number passes through one. This change of shape appears to be associated with the emergence of inertia as an important effect when the rise velocity is faster than the speed at which elastic and diffusive signals can propagate (see § 7 for a brief discussion).

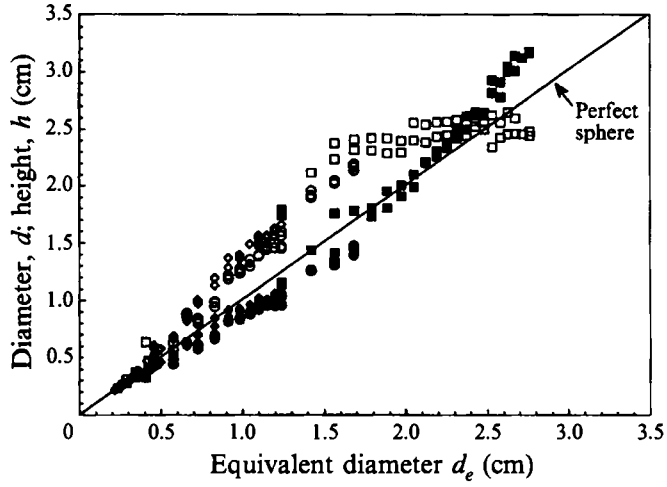


FIGURE 8. The relation between the maximum horizontal diameter, the height and the volume of the air bubbles in 1.5% polyox in different columns: ●, ○, rectangular column 4; ◆, ◇, square column 5; ■, □, rectangular column 7. The filled symbols are for the diameters and the open symbols are for the heights.

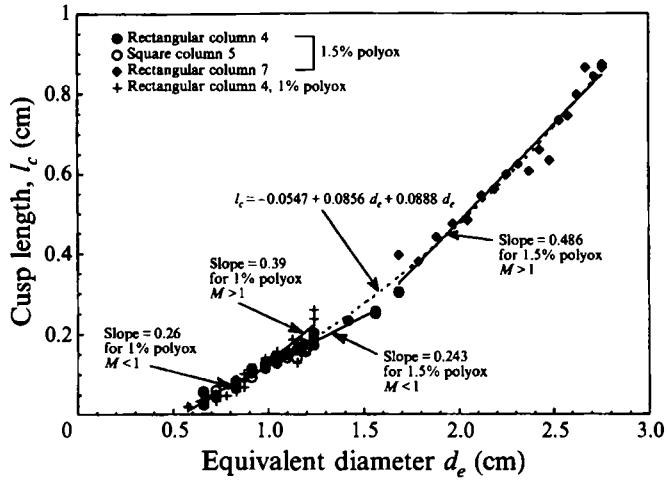


FIGURE 9. The relation between cusp length and equivalent diameter of an air bubble in 1% and 1.5% aqueous polyox solutions in various columns.

| Liquid | $d_1$ (cm) | $d_2$ (cm) | $d_3$ (cm) |
|---|---|---|---|
| 1.5% polyox | ~ 0.35 | 0.35 ~ 0.55 | ~ 1.6 |
| 1% polyox | ~ 0.3 | 0.3 ~ 0.4 | ~ 1 |

TABLE 3. The three critical equivalent diameters (volumes) corresponding to the shape changes

Values of $d_1$, $d_2$ and $d_3$ from our experiments are given in table 3. Figure 9 shows the relation between the cusp length and the bubble volume. The length of the broad edge of the two-dimensional cusp increases linearly with different slopes before and after $M = 1$, as volume increases. The slope for $M > 1$ is greater (0.39 for 1% polyox and

0.486 for 1.5% polyox) than that for $M < 1$ (0.26 for 1% polyox and 0.243 for 1.5% polyox). All the data can be fitted with the second-order polynomial as shown in figure 9.

## 4. Shape and orientation of the cusp

We present here a qualitative description of the shape and orientation of the cusped edge of gas bubbles rising in viscoelastic liquids.

### 4.1. *Shape of the cusped edge on a rising gas bubble*

When the volume of a rising air bubble in a viscoelastic fluid exceeds a critical value, a cusp will appear at the trailing edge. Photographs of the cusp edge on air bubbles rising in S1 are shown in figure 10 from two mutually perpendicular views in a rectangular column (*a*, *b*) and square column (*c*, *d*) respectively. We say that the cusped trailing edge is two-dimensional with the cusp edge shown in (*a*) and (*c*) in one direction, and the axe edge shown in (*b*) or the arrow edge shown in (*d*) in the orthogonal direction. The broad edge looks like an axe edge (shown in *b*) for smaller bubble volumes and like an arrow edge (shown in *d*) when the bubble volume is large relative to the column cross-section. Hassagar's (1979) picture shows a flat spade edge. A guillotine edge, sketched in figure 12 below, arises in the hole in a free surface pulled down by flow into a sink below. Such an edge might occur in a gas bubble held stationary by continuous withdrawing of the liquid in which it would otherwise rise.

Air bubbles rising freely in a Newtonian liquid do not cusp. However, when the column is tilted to certain angles a cusp tail may appear when an air bubble rises against the inclined wall (see §6 for details).

The two-dimensional cusping of rising air bubbles appears to depend on the fluid and the bubble volume, and is independent of the size or shape of the bubble column. Cusps were observed under very similar conditions in every column listed in table 1. This is a qualitative characterization; details of the cusp formation, the critical volume and the orientation of the cusp edge are affected by the geometry of the column. A cusp-like formation at the trailing edge of an air bubble rising in a round column filled with a 1.5% solution of polyox in water is shown in figure 11.

Two-dimensional cusps were observed in all the aqueous polyox solutions we tested. These liquids shear thin and develop high normal stresses in shear. Two-dimensional cusps are also observed on air bubbles in S1 and STP. The S1 solution shear thins at low and moderate shear rates but it develops large normal stresses at the same shear rate. STP is a Boger fluid with only small normal stresses in the interval of shear rates for which the viscosity is almost constant. We do not know the precise properties of a viscoelastic fluid which cause it to cusp in such a peculiarly asymmetric way, but the cusp configuration is compelling evidence for stretching in extension.

Another cusp shape can be produced on the free surface of a polymeric liquid in sink flow. This is like a stationary bubble which rises in a falling liquid. The sink flow experiment was done first by Gordon & Balakrishnan (1972) and is described by Bird *et al.* (1987) as follows:

> ... The experiment is done by first filling a large tank with water, stirring the water to generate a circulation in the tank, and finally removing a plug from the center of the bottom to allow the water to drain. As the water empties from the tank, a very stable air core reaching all the way to the outlet forms, accompanied by a pronounced slurping sound. Now, if a very small amount of certain polymers is added to the draining water, the air core suddenly disappears and the noise that goes with it ceased....

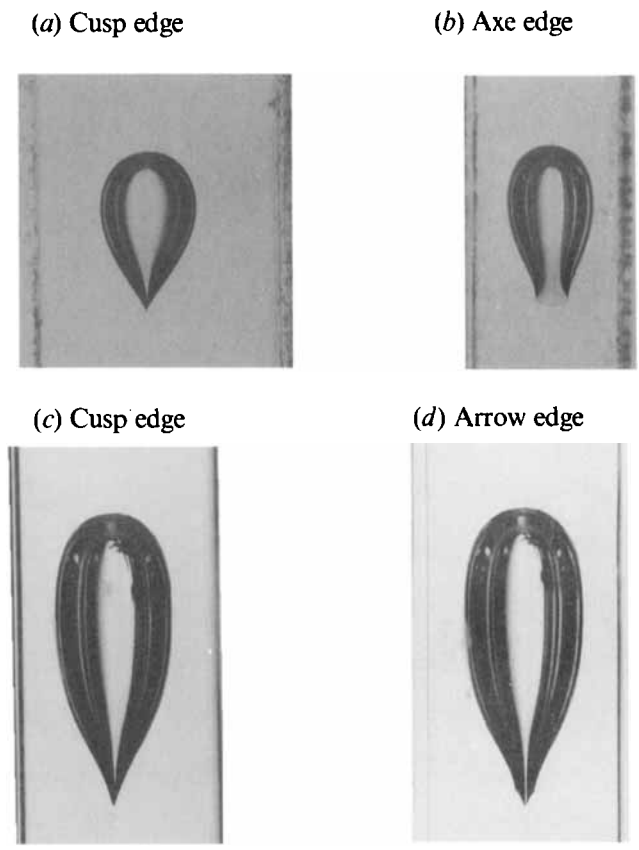


FIGURE 10. Cusped air bubbles rising in S1. (*a*) A 2 cm³ bubble photographed from the wide side of the rectangular bubble column 1. (*b*) Photographed from the narrow side of column 1. (*c*), (*d*) Photographs of a 6 cm³ bubble in the square bubble column 2 from mutually perpendicular directions.

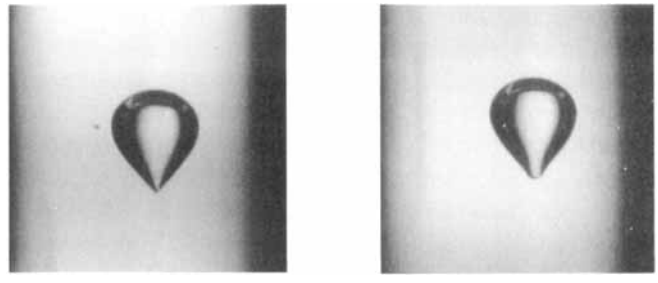

FIGURE 11. An air bubble of volume 0.5 cm³ rising in a 1.5% solution of polyox in water. The photographs were taken from two mutually perpendicular directions in round column 6.

We did similar experiments, except that we made no attempt to produce a pre-existing swirl, since local rotations already in the liquid amplify strongly as the fluid is drawn into the vortex, as in a bathtub vortex. Our experiment was carried out in a container with a square cross-section, $10 \times 10 \times 15$ in., which is shown in a cartoon form in figure 12. In sink flow of a Newtonian fluid, a very stable air core goes all the way down to the outlet from the liquid free surface. However if the liquid is viscoelastic, then the air core is cut off at a short distance from the free surface. This

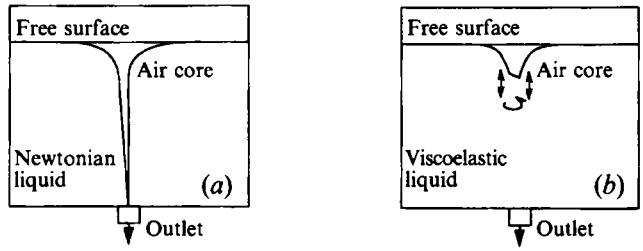


FIGURE 12. Sink flow of (*a*) a Newtonian liquid and (*b*) a viscoelastic liquid. In the viscoelastic case, an inclined two-dimensional cusp with a guillotine edge develops at the place where the air core disappears. This cusp rotates around its axis as it fluctuates up and down. We could imagine this cusp on an air bubble held in place by withdrawing liquid.

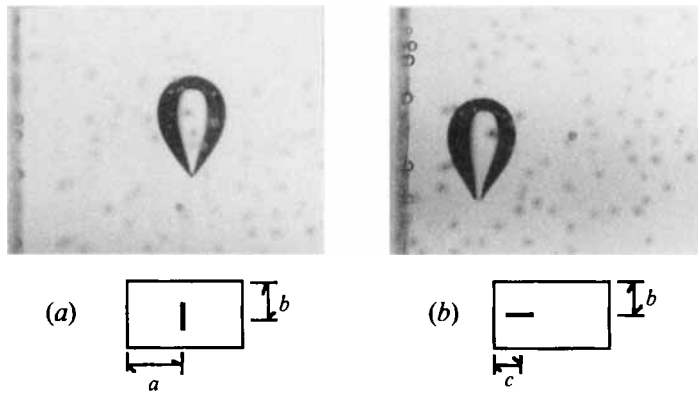


$a = 0.75$ in., $b = 0.5$ in., $c < b$

FIGURE 13. The effect of the proximity of sidewall on the orientation of the broad edge of a cusped 0.4 cm$^3$ bubble in 1.5% aqueous polyox. (*a*) The bubble is centred with a broad edge parallel to the narrow wall. (*b*) The bubble is moved to the left wall and the cusped edge rotates through 90°. The stable orientation of the cusp edge in regime 1 is such that the broad edge is perpendicular to the closest wall.

phenomenon is called vortex inhibition. What is new here is that at the place where the air core is cut off there is a two-dimensional cusp. The edge of this two-dimensional cusp looks like a guillotine edge and instead of being parallel to the free surface, it is inclined. The orientation of the guillotine edge is not fixed; it rotates around its axis and fluctuates up and down as indicated by the arrows in figure 12(*b*). The length of the guillotine edge in a 0.85% aqueous polyox solution is about 1/3 of the outlet diameter.

### 4.2. *Orientation of the cusp edge relative to the sidewall*

The orientation of a two-dimensional cusp relative to the sidewall of a rectangular column can be classified into three regimes. There is no special orientation of the cusp edge when the effects of the sidewalls of the column are minimal, that is when the column cross-section is round or the wall is far away from the rising bubble.

*Regime 1* The broad edge is parallel to the narrow window of a rectangular column. If the column is rectangular and the terminal velocity is low, the broad edge of the cusp will always be seen from the narrow window of the column and the sharp edge of the cusp will be seen in the wide window of the column. This regime appeared in the concentrated polyox solutions and the S1 solution but not in less viscoelastic fluid: STP or polyox solutions with weight concentrations less than 1%. Figures 6 and 10 are examples of this case.

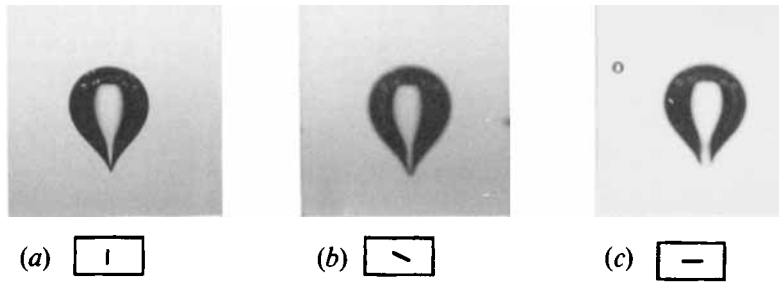


FIGURE 14. Metastable orientations in regime 2 of a 0.5 cm³ air bubble rising in 1 % solution of polyox in water in rectangular column 4: (*a*) parallel to the narrow window, (*b*) on the diagonal and (*c*) perpendicular to the narrow window. The orientation is also indeterminate when the sidewalls are far removed.

In this regime, the orientation of the two-dimensional cusp is actually controlled by the proximity of the bubble to the nearest wall. If a bubble, whose broad edge is parallel to the narrow window of the column when the bubble is in the centre of a rectangular column, is placed closer to the narrow window, then the bubble will rise with its broad edge perpendicular to rather than parallel to the narrow window, as shown in figure 13.

We may imagine a body linked to all walls by rubber bands. These bands are shortest near the closest wall and they are harder to stretch. The situation may be similar for a bubble rising in viscoelastic liquid with extensional effects dominant nearest the wall. In this case, any perturbation in orientation brings one or other side of the broad edge closer to the nearest wall where it experiences a still greater pull turning it further until the broad side is perpendicular to the wall.

*Regime 2* Large bubbles rise faster and the orientation of the cusp becomes indeterminate in square columns and even in rectangular ones. Though the two-dimensional cusp rotates about its axis in these cases, there appear to be three metastable orientations: the broad edge perpendicular to either the longer or shorter sidewalls, or across the diagonal, as shown in figure 14. The broad edge resides in one of these three orientation a little longer as it rotates. The diagonal orientation is more unstable than the other two.

*Regime 3* In this regime, the bubble volume and rise velocity are larger than in regime 2. In rectangular columns, the bubble rotates 90° from the orientation it preferred in regime 1; the cusp edge is now seen in the narrow window and the broad edge in the wide window (see figure 7). The change in orientation from regime 2 to regime 3 occurs rather suddenly as the bubble volume is increased. The critical volume for a bubble rising in a 1.5% solution of polyox in water in rectangular column 7 is about 2 cm³. The critical volume in a 1 % solution of polyox in water in column 4 is about 0.5 cm³.

The change in the orientation of the cusp in regime 3 is supercritical; it occurs when the terminal velocity is greater than the shear wave speed, $U/c = M > 1$ ($Re > 0.2$) and greater than the diffusion speed $U > 0.2\nu/d$. This change is very dramatic since the bubble rotates through 90° as in the tilt transition in which sedimenting long particles turn 90° from along the stream to across the stream as $M$ and $Re$ increase past 1 (Liu & Joseph 1993; Joseph & Liu 1993).

Another demonstration of the power of this supercritical transition can be obtained by slowing a bubble rising with $U > c$ to $U < c$ by tilting the bubble column. A 10 cm³ air bubble was formed in the 1.5% polyox solution in rectangular column 7. The rise

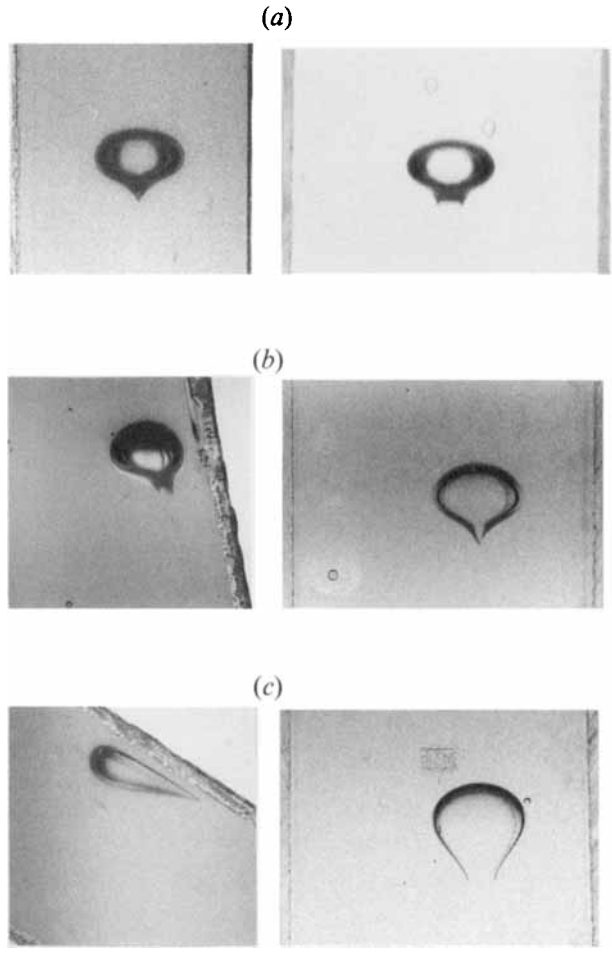


FIGURE 15. Two-dimensional cusps in inclined columns: 10 cm³ bubbles rising in 1.5% polyox in the rectangular column 7. Photographs on the left-hand side were taken from the narrow side of the column, and those on the right from the wide side. (*a*) Vertical column (supercritical), (*b*) column tilted 80° from horizontal (subcritical), (*c*) column tilted 40° from horizontal (wall dominated). The change in orientation which was caused by tilting through 80° is remarkable.

velocity $U > c$ in the vertical column was supercritical and the orientation is the characteristic one for regime 3 with the broad edge parallel to the wide window (figure 15*a*). When the column is tilted 10° from vertical the bubble rises with $U < c$ to an equilibrium near the upper wall with the broad edge characteristically perpendicular to the closest (upper) wall (figure 15*b*). An uncharacteristic orientation of the broad edge of the cusp can be seen in figure 15(*c*) for a tilt angle of 50° from vertical. In this case, the edge orientation is dominated by buoyancy which put the broad edge parallel to the close (upper) wall.

## 5. Cusping and the sudden increase of velocity

We have already remarked that cusp formation and the associated reduction of drag occur at a critical capillary number, $Ca \approx 1$ shown in figures 4(*a*) and 5. Previously published experiments designed to study the velocity jump also appear to correlate

| Liquid | Critical radius (cm) | Velocity jump (cm $s^{-1}$) | Critical capillary number | Note | Reference |
|---|---|---|---|---|---|
| 1% aqueous polyox | 0.134 | 0.5 ~ 2 | 0.61 ~ 2.44 | Estimate | Calderbank *et al.* (1970) |
| 0.3% aqueous ET497 | 0.267 | 8 ~ 17 | 0.67 ~ 1.42 | | |
| 0.7% aqueous ET497 | 0.288 | 0.8 ~ 4 | 0.53 ~ 2.67 | | |
| 0.25% aqueous J-100 | 0.271 | 7 ~ 16 | 0.58 ~ 1.33 | Estimate | Astarita & Apuzzo (1965) |
| 0.5% aqueous J-100 | 0.286 | 1.3 ~ 7 | 0.87 ~ 4.67 | | |
| 0.5% aqueous Separans AP30 | 0.281 | 2 ~ 10 | 0.67 ~ 3.33 | | |
| 1% aqueous Separans AP30 | 0.262 | 0.5 ~ 2 | 0.83 ~ 3.33 | Accurate | Leal *et al.* (1971) |
| 1% aqueous CMC | 0.243 | 1.3 ~ 3 | 0.87 ~ 2 | | |
| 0.75% aqueous CMC | 0.229 | 12 ~ 20 | 0.8 ~ 1.33 | | |
| 0.1% aqueous CMC | 0.193 | 13 ~ 25 | 0.65 ~ 1.25 | | |
| 0.5% PAA in glycerin | 0.235 | 0.8 ~ 2 | 0.63 ~ 1.59 | Estimate | Acharya *et al.* (1977) |
| 0.5% aqueous PAA | 0.235 | 1.2 ~ 2.3 | 0.9 ~ 1.72 | | |
| 0.5% aqueous PEO | 0.235 | 1.4 ~ 3.5 | 0.93 ~ 2.33 | | |
| 1% aqueous polyox | 0.165 | 0.3 ~ 0.8 | 0.38 ~ 1.02 | | |
| 1.5% aqueous polyox | 0.275 | 0.05 ~ 0.5 | 0.14 ~ 1.44 | Accurate | Present work |

TABLE 4. Critical values for cusp formation and rapid increase of the terminal velocity

with a critical capillary number of order one. We calculated critical capillary numbers for the jump rise in velocity in the literature. These values and the values from our experiments are listed in table 4.

Critical capillary numbers ranging between 0.48 and 9.24 for many different Newtonian and non-Newtonian liquids were found on the free surface cusp studied by Joseph *et al.* (1991) and Jeong & Moffatt (1992). These cusps were generated by two counter-rotating rollers submerged in the fluid which produce plunging flows which draw the free surface into a cusp. These studies also constructed analyses of the cusping of a free surface in models of the experiments. A local analysis of Stokes flow by Joseph *et al.* (1991) showed that if surface tension is zero, then the cusp shape is given by $y = ax^{2/3}$. A similar analysis of Joseph (1992) showed that the same generic form cusp singularity satisfied the local problem for a second-order fluid with inertia neglected. In a more comprehensive and global analysis of another model, Jeong & Moffatt (1992) showed that if surface tension is small but not zero a 'pseudo cusp' with a small tip radius will form. The radius of such a tip is an exponential function of the capillary number and is of the order of angstroms when the capillary number is order one. Such rounding is a negligible perturbation of $y = ax^{2/3}$ where the exponent does not change. In fact the results imply that intermolecular forces neglected in the analysis will always

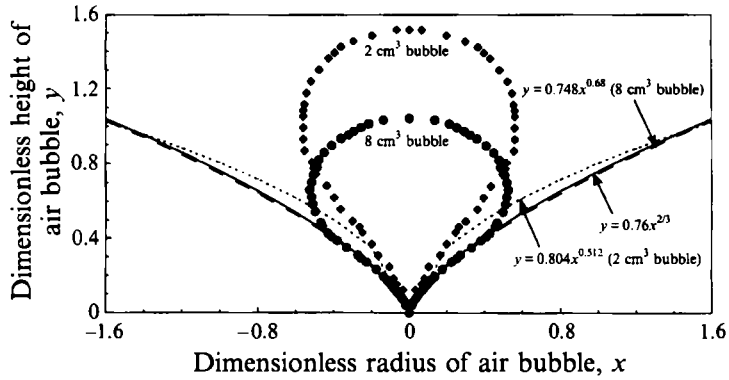


FIGURE 16. Analytic approximations of the cusp shape for the 2 cm³ and 8 cm³ bubbles shown in figure 7. The radius and height of the bubbles are made dimensionless with their equivalent diameters. The cusp is fitted to a power law whose index increases asymptotically to 2/3 as the bubble volume increases.

come into play at a 'pseudo cusp' tip and disjoining pressure could collapse the rounded tip as happens for real bubbles of small diameter.

In view of the results just given and the arguments leading to equation (1) we might wonder if $y = ax^{2/3}$ is the universal asymptotic form for all free surfaces which give rise to two-dimensional cusps.

In the case of rising bubbles it is not possible to resolve the shape of the singular tail at small volumes (see figure 6). Nonetheless, we can carry out a power-law fitting for the bubbles in figure 7. The power laws do not represent the shape of the bubbles in the tip region accurately when the bubble is small, but for large bubbles the index increases asymptotically to 2/3 (see figure 16). Similar results hold for other cusping bubbles; they all give rise to $y = ax^{2/3}$ asymptotically.

The appearance of cusps in gas bubbles rising in viscoelastic liquids at capillary numbers of the same order, $O(1)$, as in viscous liquids is strange because the capillary number expresses a balance between surface tension and viscous forces; the viscoelasticity is not included. This unexpected dependence on a capillary number was noted by Joseph *et al.* (1991) and they constructed an argument to show that the capillary number criterion also applies to a second-order fluid. The experiments are much more convincing than the argument so that the question remains to be answered.

## 6. Cusping of a rising gas bubble in a Newtonian liquid

Cusps never form at the tail of gas bubbles rising freely in a Newtonian liquid even when the capillary number based on the rise velocity is greatly in excess of 1. However the trailing ring edge of spherical cap bubbles which form when the rise velocity is very large is cusp like and conceivably could actually cusp if the flow were laminar and the ring edge were not prey to capillary instability. The rise velocity of a spherical cap bubble corresponds to a shearing motion that could pull out a cusp so that the choice of which $U$ to use in a capillary number criterion depends on the underlying fluid dynamics.

Another way to get a rising gas bubble to cusp is to shear it against a tilted wall. An air bubble does not cusp in glycerin as it rises freely in a vertical column; in fact, the rear portion of the bubble will be flatter than its spherical front (figure 17*a*). But when

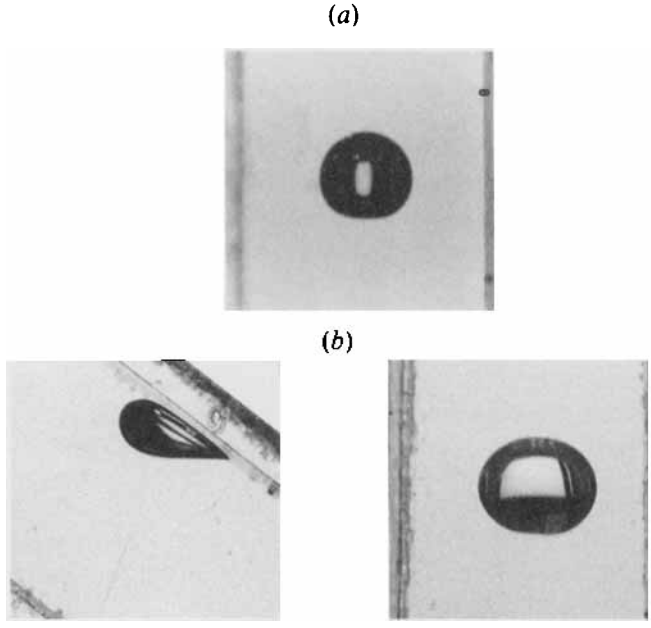


FIGURE 17. An air bubble rising in glycerin in a vertical column does not cusp (see *a* for a 0.45 cm³ bubble), but it does cusp when it is sheared against a tilted wall with tilt angle between 20° and 75°, as shown in (*b*) for a 1 cm³ bubble rising in a 45° tilted column.

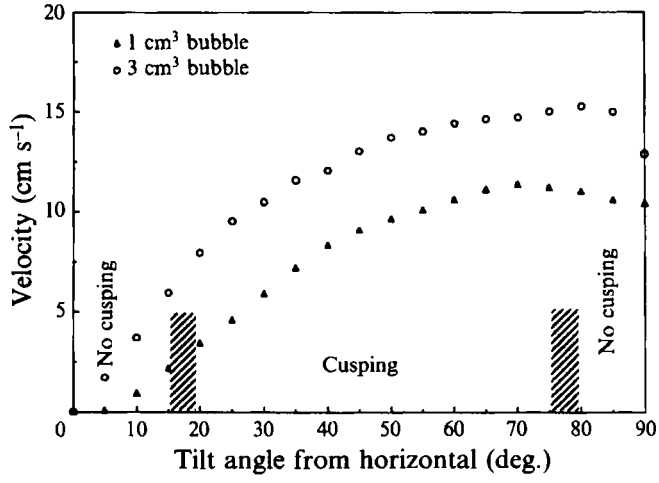


FIGURE 18. Rise velocity of air bubble versus tilt angle of the column in a square column filled with pure glycerin.

the column is tilted at any angle between 20° and 75° the bubble cusps as it rises against the inclined top wall (figure 17*b*).

The velocities of a 1 cm³ and a 3 cm³ air bubble rising in pure glycerin in the square column 5 were measured as a function of tilt angle. The results are presented in figure 18. At the highest cusping angle (75–80°), the rise velocity is maximum. The capillary numbers for cusping range from 0.5 to 2.6 for the 1 cm³ bubble and from 0.5 to 3.5 for the 3 cm³ bubble. These values are close to the critical value ($Ca = 2.62$) found by

Joseph *et al.* (1991) in the case of rotating cylinders. In fact, the bubble rising against a tilted wall alone is equivalent to a stationary bubble pulled into a cusp by a plunging wall which is the basic cusping device in the rotating cylinder experiments.

## 7. Discussion and conclusions

We shall interpret the observations of transition at $M = 1$ as a change of type of the kind that is observed for flow over bodies (Joseph 1990) and in problems of sedimentation and particle migration by Liu & Joseph (1993), Joseph & Liu (1993, 1995).

The idea of a change of type has to do with the propagation of signals. In the supercritical case the body rises faster than the signals. A signal can propagate by a shear wave, so $U > c$ ($M > 1$), and by diffusion, so $U > 0.2\nu/d$ ($Re > 0.2$). In this case the fluid above senses the motion immediately through the presure as in potential flow. This may be why the fronts of large gas bubbles look alike in Newtonian and viscoelastic fluids even when their back sides are different. We made some observations of bubbles rising in 0.85% aqueous polyox in the square bubble column 10: when $M > 1$ and the Reynolds number is large the bubble develops a lenticular shape as in Newtonian liquid but with a little tail at the rear.

A summary list of the results obtained in this paper is as follows:

(i) Cusped tails abruptly form on air bubbles rising in polymeric liquids with capillary numbers near unity.

(ii) The cusped tail is basically two-dimensional with a broad edge in one view and a sharp cusped edge in the orthogonal view. The flow corresponding to the two-dimensional cusp can be considered like a biaxial extension expanding the broad edge and the long axis of the bubble and contracting the sharp edge. Axisymmetric cusp shapes are never observed.

(iii) The shape of the broad edge may be like a spade, an axe, an arrow, or a guillotine blade. The guillotine blade arises in a sink flow of a viscoelastic liquid at the place near the dimple on the free surface where the core terminates (vortex inhibition). This dimple is actually a two-dimensional guillotine cusp which rotates around its axis and fluctuates up and down. We tested the form of the generic analytic cusp tip by fitting $a$ and $n$ in the expression $y = ax^n$ to measured values for even larger bubble volumes in which the cusp-like shape of the tail was even more in evidence. We found that $n = 2/3$, consistent with the form of a generic analytic cusp.

(iv) The rapid cusping of a rising bubble for small increases of volume near a critical capillary number is also manifested in a rapid rise in the terminal velocity which has been recorded by previous experimenters. The jump in velocity occurs when the cusp appears and it can be as much as ten fold.

(v) The orientation of the broad edge of a cusped bubble near a plane wall is evidently determined by the properties of the fluid and flow in very particular ways. Roughly speaking, when the viscoelastic Mach number is less than 1 in a strong viscoelastic liquid, the broad edge aligns itself perpendicular to a close wall; any deviation from this perpendicular orientation is unstable and the bubble will turn its broad edge perpendicular so that the profile of the sharp edge is seen through the wall. On the other hand, when the viscoelastic Mach number is greater than 1, the broad edge parallel to the close wall is stable and the perpendicular orientation is unstable. The orientation properties are summarized in the case of centred bubbles rising in rectangular columns by the statement that the sharp edge can be seen in the wide window when $M < 1$ and in the narrow window when $M > 1$. The orientation is

indeterminate near $M = 1$, or when the cross-section is circular, or when the sidewalls are further away, or when the liquid is less viscoelastic. Orientations perpendicular to walls are metastable when they are not stable and there is also a weaker tendency for the broad edge to align along the diagonal.

(vi) The changes of the shape of an air bubble as it rises in a viscoelastic fluid are rapid, but smooth near the point of cusping. The change of shape from convex to concave near the tail of the bubble is very localized at first so that the determination of the exact shape at the tail has not been done. For large bubble volumes the cusp shape is evident in one view and the axe shape in the perpendicular view. Still larger volumes give rise to an arrow edge. We measured the growth in the length of the axe edge and found it to be linear in the bubble volume when $M < 1$ and linear but with a different slope when $M > 1$.

(vii) There is a change in the slope of rise velocity versus bubble volume for $M > 1$ corresponding to an increase in the lateral spreading of the bubble as is consistent with the dominating effect of inertia when $M > 1$. The Deborah number increases with bubble volume when $M < 1$ but is flat when $M > 1$ so that the balance between buoyancy and drag which gives rise to $U \propto d^2$ for $M < 1$ changes to $U \propto d$ for $M > 1$.

(viii) Air bubbles which rise along tilted walls are dominated by that wall and the broad edge of the cusp will always lie parallel to the wall if the tilt angle from horizontal is small enough. The walls of our columns were always wet by liquid so that the rise of the air bubble near a tilted wall is equivalent to the plunging of a plate coated with liquid into air. The cusp that forms here is like that produced by the rotating cylinders used by Joseph *et al.* (1991) and by Jeong & Moffatt (1992). We found that air bubbles cusped in glycerin in this tilted configuration in an interval of tilt angles with capillary numbers ranging from 0.5 to 3.5, consistent with the earlier results.

This work was supported by the NSF, Fluid, Particulate and Hydraulic Systems, by the US Army, Mathematics, and by the DOE, Department of Basic Energy Sciences.

## REFERENCES

ACHARYA, A., MASHELKAR, R. A. & ULBRECHT, J. 1977 Mechanics of bubble motion and deformation in non-Newtonian media. *Chem. Engng Sci.* **32**, 863–872.

ASTARITA, G. & APUZZO, G. 1965 Motion of gas bubbles in non-Newtonian liquids. *AIChE J.* **11**, 815–819.

BARNETT, S. M., HUMPHEREY, A. E. & LITT, M. 1966 Bubble motion and mass transfer in non-Newtonian fluids. *AIChE J.* **12**, 253.

BHAGA, D. & WEBER, M. E. 1981 Bubbles in viscous liquids: shapes, wakes and velocities. *J. Fluid Mech.* **105**, 61–85.

BIRD, R. B., ARMSTRONG, R. C. & HASSAGER, O. 1987 *Dynamics of Polymeric Liquids*, 2nd Edn, Vol. 1. John Wiley & Sons.

BISGAARD, C. 1983 Velocity fields around spheres and bubbles investigated by laser-Doppler anemometry. *J. Non-Newtonian Fluid Mech.* **12**, 283–302.

BISGAARD, C. & HASSAGER, O. 1982 An experimental investigation of velocity fields around spheres and bubbles moving in non-Newtonian liquids. *Rheol. Acta* **21**, 537–539.

CALDERBANK, P. H. 1967 Review series No. 3 – Gas absorption from bubbles. *Trans. Inst. Chem. Engrs* **45**, 209.

CALDERBANK, P. H., JOHNSON, D. S. L. & LOUDON, J. 1970 Mechanics and mass transfer of single bubbles in free rise through some Newtonian and non-Newtonian liquids. *Chem. Engng Sci.* **25**, 235–256.

CHILCOTT, M. D. & RALLISON, J. M. 1988 Creeping flow of dilute polymer solutions past cylinders and spheres. *J. Non-Newtonian Fluid Mech.* **29**, 381–432.

CLIFT, R., GRACE, J. R. & WEBER, M. 1978 *Bubbles, Drops and Particles.* Academic.

COUTANCEAU, M. & HAJJAM, M. 1982 Viscoelastic effect on the behavior of an air bubble rising axially in a tube. *Appl. Sci. Res.* **38**, 199–207.

DE KÉE, D., CARREAU, P. J. & MORDARSKI, J. 1986 Bubble velocity and coalescence in viscoelastic liquids. *Chem. Engng Sci.* **41**, 2273–2283.

FARAROURI, A. & KINTNER, R. C. 1961 Flow and shape of drops in non-Newtonian fluids. *Trans. Soc. Rheol.* **5**, 369–380.

FENG, J., JOSEPH, D. D., GLOWINSKI, R. & PAN, T. W. 1995 A three-dimensional computation of the force and moment on an ellipsoid settling slowly through a viscoelastic fluid. *J. Fluid Mech.* **283**, 1–16.

GARNER, F. H., MATRUS, K. B. & JENSEN, V. G. 1957 Distortion of fluid drops in the Stokesian region. *Nature* **180**, 331.

GORDON, R. J. & BALAKRISHNAN, C. 1972 Vortex inhibition: a new viscoelastic effect with importance in drag reduction and polymer characterization. *J. Appl. Polymer Sci.* **16**, 1629–1639.

HASSAGER, O. 1979 Negative wake behind bubbles in non-Newtonian liquids. *Nature* **279**, 402–403.

HASSAGER, O. 1985 The motion of viscoelastic fluids around spheres and bubbles. In *Viscoelasticity and Rheology* (ed. A. S. Lodge, M. Renardy & J. A. Nohel). Academic.

JEONG, J. & MOFFATT, H. K. 1992 Free-surface cusps associated with flow at low Reynolds number. *J. Fluid Mech.* **241**, 1—22.

JOSEPH, D. D. 1990 *Fluid Dynamics of Viscoelastic Liquids.* Springer.

JOSEPH, D. D. 1992 Understanding cusped interfaces. *J. Non-Newtonian Fluid Mech.* **44**, 127–148.

JOSEPH, D. D. & FENG, J. 1995 The negative wake in a second-order fluid. *J. Non-Newtonian Fluid Mech.* **57**, 313–320.

JOSEPH, D. D. & LIU, Y. J. 1993 Orientation of long bodies falling in a viscoelastic liquid. *J. Rheol.* **37**, 961–983.

JOSEPH, D. D. & LIU, Y. J. 1995 Motion of particles settling in a viscoelastic fluid. *Proc. 2nd Intl Conf. on Multiphase Flow, Kyoto, Japan, April 3–7* (ed. A. Serizawa, T. Fukano & J. Bataille).

JOSEPH, D. D., LIU, Y. J., POLETTO, M. & FENG, J. 1994 Aggregation and dispersion of spheres falling in viscoelastic liquids. *J. Non-Newtonian Fluid Mech.* **54**, 45–86.

JOSEPH, D. D., NELSON, J., RENARDY, M. & RENARDY, Y. Y. 1991 Two-dimensional cusped interfaces. *J. Fluid Mech.* **223**, 383–409.

JOSEPH, D. D. & RENARDY, Y. Y. 1993 *Fundamentals of Two-Fluid Dynamics.* Springer.

LEAL, L. G., SKOOG, J. & ACRIVOS, A. 1971 On the motion of gas bubbles in a viscoelastic liquid. *Can. J. Chem. Engng* **49**, 569–575.

LIU, Y. J. & JOSEPH, D. D. 1993 Sedimentation of particles in polymer solutions. *J. Fluid Mech.* **255**, 565–595.

MHATRE, M. V. & KINTNER, R. C. 1959 Fall of liquid drops through pseudoplastic liquids. *Ind. Engng Chem.* **51**, 865.

NOH, D. S., KANG, I. S. & LEAL, L. G. 1993 Numerical solutions for the deformation of a bubble rising in dilute polymeric fluids. *Phys. Fluids* A **5**, 1315–1332.

PHILIPPOFF, W. 1937 The viscosity characteristics of rubber solutions. *Rubber Chem. Tech.* **10**, 76.

SIGLI, S. & COUTANCEAU, M. 1977 Effect of finite boundaries on the slow laminar isothermal flow of a viscoelastic fluid around a spherical obstacle. *J. Non-Newtonian Fluid Mech.* **2**, 1–22.

WARSHAY, M. E., BOGUSZ, E., JOHNSON, M. & KINTNER, R. C. 1959 Ultimate velocity of drops in stationary liquid media. *Can. J. Chem. Engng* **37**, 29.

ZANA, E. 1975 PhD thesis, California Institute of Technology.

ZANA, E. & LEAL, L. G. 1978 The dynamics and dissolution of gas bubbles in a viscoelastic fluid. *Intl J. Multiphase Flow* **4**, 237.